ELSEVIER

Photonic band structure for a superconductor-dielectric superlattice

Chien-Jang Wu [a,*], Mei-Soong Chen [b], Tzong-Jer Yang [b]

[a] *Department of Applied Physics, National University of Kaohsiung, Kaohsiung 811, Taiwan, ROC*
[b] *Department of Electrophysics, National Chiao-Tung University, Hsinchu 300, Taiwan, ROC*

Abstract

The photonic band structure in the transversal electric mode for a one-dimensional superconductor-dielectric super-lattice is theoretically calculated. By using the Abeles theory for a stratified medium, we first calculate the transmittance spectrum from which all the possible bands can be directly seen. Then we calculate the real photonic band structure based on the transcendental equation derived from the transfer matrix method and Bloch theorem. The band structure is shown to be strongly consistent with the transmittance spectrum. We finally study the three lowest band gaps as a function of penetration of superconductor, permittivity of dielectric, and angle of incidence, respectively. The optical properties in a superconductor-dielectric superlattice thus are well disclosed.
© 2005 Elsevier B.V. All rights reserved.

1. Introduction

It is well known that photonic crystals have photonic band gaps (PBGs) in the photonic dispersion relation. In the PBGs, optical waves with certain frequencies are not allowed to propagate

through the crystal [1,2]. The PBGs are analogous to the electronic band gaps in a solid and their physical origin can be ascribed to the Bragg diffraction in a periodic multilayer structure. A simple one-dimensional photonic crystal is, in general, made of alternating layers of material with different permittivities, forming a superlattice with infinite periods. The band structure for a dielectric–dielectric photonic crystal shows that the PBG between the first and second bands

---

* Corresponding author. Tel.: +886 7 5917476; fax: +886 7 5919357.

E-mail address: cjwu@nuk.edu.tw (C.-J. Wu).

widens considerably as the difference in dielectric permittivity is increased [3]. In addition, no low-frequency band gap below the first (lowest) band can be found. In a metallic photonic made of a normal metal and a dielectric, it is however found that a low-frequency (or metallicity) gap may exist. Contrary to a PBG, this metallicity gap which does not depend on the periodicity, is of the order of the plasma frequency and thus is regarded as a modified effective plasma frequency [4–6].

On the other hand, studies of photonic crystals consisting of a superconducting material and a dielectric have also been reported recently [7–9]. The electromagnetic properties of Abrkosov vortex lattice as a photonic crystal were investigated by changing the Ginzburg–Landau parameter and static magnetic field [7]. In addition to a low-frequency band gap below the first band, they also obtained the PBGs for a superconductor in the presence of vortices. In fact, the issue of a superconducting photonic crystal was first investigated by a group in Singapore [8,9]. They considered a one-dimensional superconductor-dielectric superlattcie. By making use of the transfer matrix method accompanied by the Bloch theorem [10], a low-frequency band gap was seen for both transversal magnetic (TM) and transversal electric (TE) modes. This band gap was found to be about one third of the threshold frequency of a bulk superconducting material. The physical information from this work for TE mode however is quite limited because only the first band is given. As for the other higher bands in addition to the possible PBGs cannot be obtained there. In other words, a full band structure for this one-dimensional superconducting photonic crystal remains unavailable thus far.

A full band structure is a basic and important means for understanding the fundamental physics about electromagnetic wave propagation characteristics in a photonic crystal. This information is not only of fundamental but also of technical use for a superconducting material. Motivated by this, in this paper we shall extend the work of Ref. [8]. We would like to present the full photonic band structure for TE mode in a superconductor-dielectric photonic crystal. Firstly, we use the Abeles theory for a stratified media to calculate the fre-

quency-dependent transmittance [11]. From the transmittance spectrum, we can clearly learn the locations of all possible pass bands and stop bands. With these in hand, one is able to calculate the band structure from the transcendental equation based on the transfer matrix method together with the Bloch theorem. Then a comparison between the transmittance spectrum and full band structure will be made.

The format of this work is as follows: Section 2 describes the theoretical approaches to be used in the calculation. The calculated transmittance spectrum and band structure will be given in Section 3. Discussion on the PGBs will also be made in Section 3. A summary will be addressed in Section 4.

2. Theory

A one-dimensional nonmagnetic superconductor-dielectric photonic crystal will be modeled as a periodic superconductor-dielectric multilayer structure with a large number of periods, $N \gg 1$. Such an N-period superlattice is shown in Fig. 1, where $a = a_2 + a_3$ is the spatial periodicity, where a_2 is the thickness of the superconducting layer and a_3 denotes the thickness of the dielectric layer. We consider that a TE wave is incident at an angle θ_1 from the top medium which is taken to be free space with a refractive index, $n_1 = 1$. The index of refraction of the lossless dielectric is given by $n_3 = \sqrt{\varepsilon_{r3}}$, where ε_{r3} is its relative permittivity. For the superconductor, the index of refraction can be described on the basis of the conventional two-fluid model [11]. According to the two-fluid model the electromagnetic response of a superconductor can be described in terms of the complex conductivity, $\sigma = \sigma_1 - j\sigma_2$, where the real part, σ_1, indicating the loss, is contributed by the normal electrons, whereas the imaginary part, σ_2, is due to the superelectrons. The imaginary part is expressed as [12]

$$\sigma_2 = \frac{1}{\omega \mu_0 \lambda_L^2}, \tag{1}$$

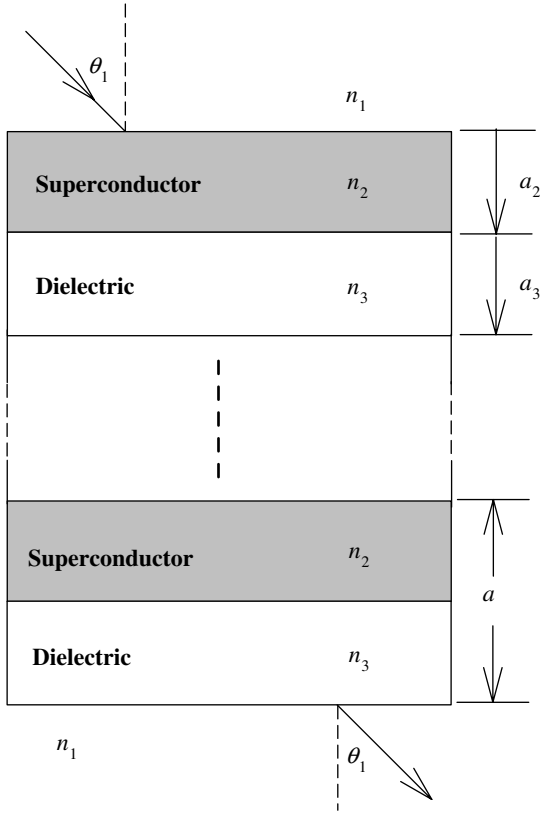where the temperature-dependent penetration depth is given by

Fig. 1. A superconductor-dielectric periodic layered structure under consideration in this paper. A transversal electric mode optical wave is incident obliquely from the top medium at an angle of incidence θ_1 on the plane superconductor boundary. The media are characterized by distinct indices of refraction n_1, n_2, and n_3, respectively. The period is a and the thicknesses of superconductor and dielectric layers are denoted by a_2, and a_3, respectively.

where the Gorter–Casimir expression for $f(T)$ is given by

$$f(T) = \left(\frac{T}{T_c}\right)^4. \tag{3}$$

We shall consider the lossless case, meaning that the real part of the complex conductivity of the superconductor can be neglected and consequently it becomes

$$\sigma = -j\sigma_2 = -j\frac{1}{\omega\mu_0\lambda_L^2}. \tag{4}$$

The conditions for a lossless superconductor are well described in Ref. [8]. With Eq. (4), the relative permittivity as well as its associated index of refraction can be obtained, namely

$$\varepsilon_{r2} = 1 - \frac{c^2}{\omega^2\lambda_L^2} \tag{5}$$

and

$$n_2 = \sqrt{\varepsilon_{r2}} = \sqrt{1 - \frac{c^2}{\omega^2\lambda_L^2}}. \tag{6}$$

In order to calculate the transmittance and reflectance for a periodic multilayered structure, the elegant Abeles theory will be employed [11]. According to this theory, we must, in advance, set up the characteristic matrix corresponding to one period, with the result

$$\mathbf{M}(a) = \begin{bmatrix} m_{11} & m_{12} \\ m_{21} & m_{22} \end{bmatrix} = \begin{bmatrix} \cos\beta_2 & \dfrac{j}{p_2}\sin\beta_2 \\ jp_2\sin\beta_2 & \cos\beta_2 \end{bmatrix} \begin{bmatrix} \cos\beta_3 & \dfrac{j}{p_3}\sin\beta_3 \\ jp_3\sin\beta_3 & \cos\beta_3 \end{bmatrix}$$

$$= \begin{bmatrix} \cos\beta_2\cos\beta_3 - \dfrac{p_3}{p_2}\sin\beta_2\sin\beta_3 & \dfrac{j}{p_3}\cos\beta_2\sin\beta_3 + \dfrac{j}{p_2}\sin\beta_2\cos\beta_3 \\ jp_2\sin\beta_2\cos\beta_3 + jp_3\cos\beta_2\sin\beta_3 & \cos\beta_2\cos\beta_3 - \dfrac{p_2}{p_3}\sin\beta_2\sin\beta_3 \end{bmatrix}, \tag{7}$$

$$\lambda_L = \lambda_L(T) = \frac{\lambda_0}{\sqrt{1 - f(T)}}, \tag{2}$$

where

$$\beta_2 = \frac{2\pi}{\lambda_0}n_2a_2\cos\theta_2, \quad \beta_3 = \frac{2\pi}{\lambda_0}n_3a_3\cos\theta_3 \tag{8}$$

and

$$p_2 = \sqrt{\frac{\varepsilon_0}{\mu_0}} n_2 \cos\theta_2, \quad p_3 = \sqrt{\frac{\varepsilon_0}{\mu_0}} n_3 \cos\theta_3, \qquad (9)$$

where $\lambda_0 = 2\pi/k_0 = 2\pi c/\omega$ is the wavelength in free space. The angles θ_2 and θ_3, determined by Snell's law of refraction, are the ray angles in layer 2 and 3, respectively. Having constructed the matrix in Eq. (7), the total characteristic matrix for an N-period structure can be obtained, that is

$$[\mathbf{M}(Na)] = \begin{bmatrix} M_{11} & M_{12} \\ M_{21} & M_{22} \end{bmatrix} = [\mathbf{M}(a)]^N$$

$$= \begin{bmatrix} m_{11} U_{N-1}(\Psi) - U_{N-2}(\Psi) & m_{12} U_{N-1}(\Psi) \\ m_{21} U_{N-1}(\Psi) & m_{22} U_{N-1}(\Psi) - U_{N-2}(\Psi) \end{bmatrix}, \qquad (10)$$

where

$$\Psi = \frac{1}{2}(m_{11} + m_{22}) \qquad (11)$$

and U_N are the Chebyshev polynomials of the second kind defined by

$$U_N(\Psi) = \frac{\sin[(N+1)\cos^{-1}\Psi]}{\sqrt{1-\Psi^2}}. \qquad (12)$$

Eq. (10) gives the explicit expressions for matrix elements M_{11}, M_{12}, M_{21}, and M_{22} as follows:

$$M_{11} = \left(\cos\beta_2 \cos\beta_3 - \frac{p_3}{p_2}\sin\beta_2\sin\beta_3\right) U_{N-1}(\Psi) - U_{N-2}(\Psi),$$

$$M_{12} = j\left(\frac{1}{p_3}\cos\beta_2\sin\beta_3 + \frac{1}{p_2}\sin\beta_2\cos\beta_3\right) U_{N-1}(\Psi),$$

$$M_{21} = j(p_2\sin\beta_2\cos\beta_3 + p_3\cos\beta_2\sin\beta_3) U_{N-1}(\Psi),$$

$$M_{22} = \left(\cos\beta_2\cos\beta_3 - \frac{p_2}{p_3}\sin\beta_2\sin\beta_3\right) U_{N-1}(\Psi) - U_{N-2}(\Psi). \qquad (13)$$

The reflection and transmission coefficients can be determined and are given by [11]

$$\tilde{r} = \frac{(M_{11} + M_{12}p_\ell)p_1 - (M_{21} + M_{22}p_\ell)}{(M_{11} + M_{12}p_\ell)p_1 + (M_{21} + M_{22}p_\ell)} \qquad (14)$$

and

$$\tilde{t} = \frac{2p_1}{(M_{11} + M_{12}p_\ell)p_1 + (M_{21} + M_{22}p_\ell)}. \qquad (15)$$

Here $p_1 = \sqrt{\varepsilon_0/\mu_0}(n_1\cos\theta_1)$ is for the first medium, and $p_\ell = \sqrt{\varepsilon_0/\mu_0}(n_\ell\cos\theta_\ell)$ is for the last medium. Both media here are taken to be free space.

The reflectance (reflectivity) R, transmittance (transmissivity) T and $\tilde{t}$, $\tilde{t}$ are related by

$$R = |\tilde{r}|^2, \quad T = \frac{p_\ell}{p_1}|\tilde{t}|^2. \qquad (16)$$

Thus, the transmittance spectrum, T versus ω, can be numerically illustrated, as will be seen in Section 3.

Next, we are going to briefly describe the method used in Ref. [8] for a direct calculation of the band structure in a periodic superconductor-dielectric medium. Based on the basic assumption of translational symmetry and aided by the Floquet (or Bloch) theorem together with the use of transfer matrix method, one can obtain a transcendental equation determining the band structure, namely [8,10]

$$\cos(Ka) = \cos(k_{sx}a_2)\cos(k_x a_3)$$
$$- \frac{1}{2}\left(\frac{k_x}{k_{sx}} + \frac{k_{sx}}{k_x}\right)\sin(k_{sx}a_2)\sin(k_x a_3), \qquad (17)$$

where K is the Bloch wave number,

$$k_x = \frac{\omega}{c}\sqrt{\varepsilon_{r3} - \sin^2\theta_1} \qquad (18)$$

and

$$k_{sx} = \frac{\omega}{c}\sqrt{\cos^2\theta_1 - \frac{c^2}{\omega^2\lambda_L^2}}. \qquad (19)$$

Eq. (17) can be numerically solved for ω as a function of K, yielding the so-called photonic band structure or dispersion relation. In Ref. [8], only the first band is given and thus it is not sufficient to explore the whole optical properties in a photonic crystal. In the next section, we shall give other possible higher bands. The higher bands then enable us to study the PGBs.

Before presenting the numerical results we mention that the above theoretical formulations are based on the flat interface model. This is legitimate and widely used to theoretically study the fundamental optical properties in a photonic crystal [3,10,11]. In the actual material, some interface issues such as interface roughness, lattice imperfection, and surface discontinuity may arise due to the process of a film growth. To study surface

effect on a photonic crystal, other method such as the plane-wave expansion may be employed and some works are available [13]. A study of interface effect on the photonic crystal is not our interest here.

3. Numerical results and discussion

Let us now present the numerical results according to the aforementioned equations. Two-dimensionless quantities such as $\Omega = \omega a/2\pi c$ and $\Lambda = a/2\pi\lambda_L$ will be used as usual in the analysis of photonic bands. We also define the dielectric thickness ratio as $r = a_3/a$. Fig. 2 displays the calculated transmittance spectrum (right) and the band structure (left) for the conditions of $\theta_1 = 45°$, $\varepsilon_{r3} = 15$, $\Lambda = 0.05$, $r = 1/3$, and $N = 500$. It is seen that the calculated transmission spectrum is in fairly good agreement with that of the calculated band structure. For the sake of convenience, the first six cutoff frequencies (at which $T = 0$) are denoted by Ω_i,
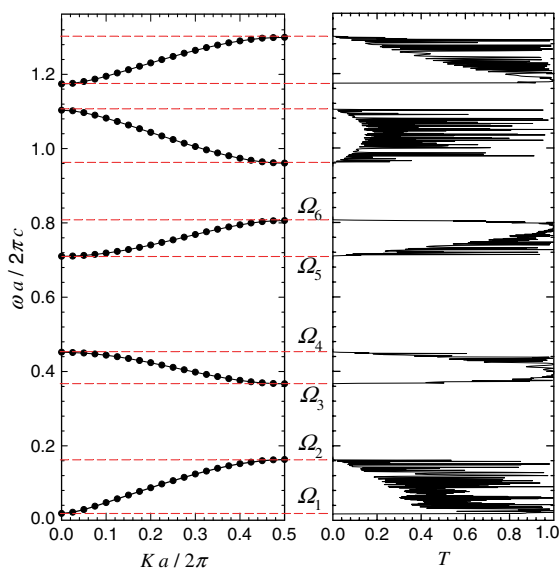

Fig. 2. The calculated transmittance spectrum (right) based on Eq. (16) and the band structure (left) calculated from Eq. (17). The horizontal dash lines mark the first six cutoff frequencies denoted by Ω_i, $i = 1, 2, 3–6$. Excellent agreement is achieved in both results. The conditions are $\theta_1 = 45°$, $\varepsilon_{r3} = 15$, $\Lambda = 0.05$, $r = 1/3$, and $N = 500$.

$i = 1, 2, 3–6$, as shown in Fig. 2. The first band gap, denoted by Δ_1, is equal to $\Omega_1 = 0.017$. The first band gap is referred to as the low-frequency (LF) gap [8], which is not seen in the dielectric–dielectric superlattice. This gap size is nearly equal to one third of the cutoff frequency Ω_c for a bulk superconductor which is in value of 0.05 here. Thus, its origin can be regarded as a combined effect of the spatial periodicity and of the addition of dielectric material [8]. The dimensionless bulk cutoff frequency $\Omega_c = 0.05$ is equal to a real frequency of $\omega_c = c/\lambda_L \sim 10^{15}\,s^{-1}$, which is of the same order of plasma frequency for most alkali metals. The dispersion relation for a bulk superconductor is thus recognized as an analogy to the plasma dispersion in metals [8]. On the other hand, Δ_1 also appears in a metallic photonic crystal but its size is near the plasma cutoff frequency, meaning that it does not depend on the periodicity [7]. Thus in the metallic superlattice Δ_1 is not a real PBG, whereas it is a true PBG in the superconductor superlattice because Δ_1 is indeed related to the periodicity.

In addition to Δ_1, along with the first band from $\Omega_1 = 0.017$ to $\Omega_2 = 0.165$, other higher bands as well as PBGs are also displayed in Fig. 2. The second PBG is denoted by Δ_2 equal to $\Omega_3 - \Omega_2 = 0.368 - 0.165 = 0.203$. That is almost twelve times larger than Δ_1. The second band is located from $\Omega_3 = 0.368$ to $\Omega_4 = 0.455$. The third PBG, Δ_3, is $\Omega_5 - \Omega_4 = 0.712 - 0.455 = 0.257$ in magnitude and is greater than Δ_2 appreciably. The third band is then above Ω_5 and under Ω_6. From the results in Fig. 2 we can deduce that the photonic band structure for a one-dimensional superconducting photonic crystal is quite reminscent of the electronic band structure. Moreover, it has multiple PGBs, instead of having just one lowest band gap as reported in Ref. [8].

Fig. 3 shows the first five cutoff frequencies and PBGs as a function of penetration depth at the conditions of $\theta = 45°$, $\varepsilon_{r3} = 15$, $r = 1/3$, and $N = 500$. The first one, Ω_1, being equal to Δ_1, increases with increasing Λ. The dependence of Δ_2 on Λ is similar to that of Δ_3. Both also increase as Λ increases. The variations in Δ_2 and Δ_3, however, are not as salient as Δ_1, especially at small values of Λ. Fig. 4 shows the calculated frequencies and PBGs as a function of angle of incidence
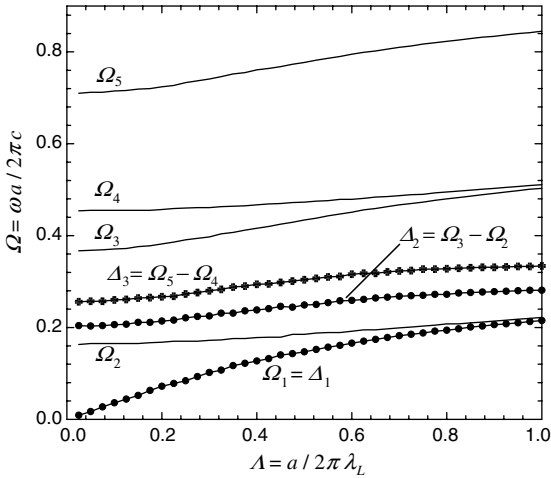
Fig. 3. Calculated five cutoff frequencies (solid lines) as well as the first three PBGs (dotted lines) as a function of penetration depth. The conditions are $\theta_1 = 45°$, $\varepsilon_{r3} = 15$, $r = 1/3$, and $N = 500$.
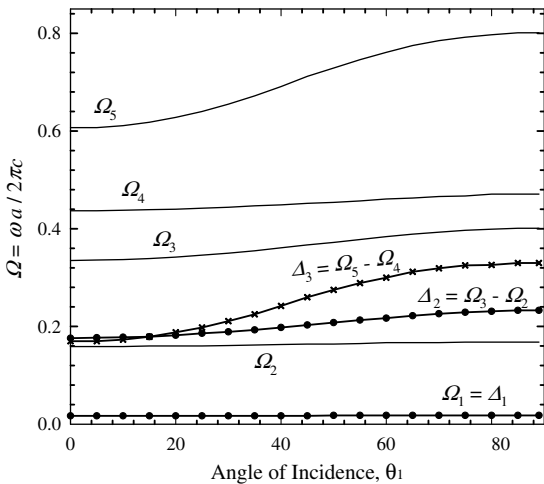

Fig. 4. Calculated five cutoff frequencies (solid lines) as well as the first three PBGs (dotted lines) as a function of angle of incidence. The conditions are $\varepsilon_{r3} = 15$, $\Lambda = 0.05$, $r = 1/3$, and $N = 500$.

at $\varepsilon_{r3} = 15$, $\Lambda = 0.05$, $r = 1/3$, and $N = 500$. It is seen that gap Δ_1 essentially does not change with the variation in the angle of incidence, indicating an omnidirectional feature. In addition, Δ_2 changes slightly as a function of angle of incidence. The change in the third gap size, Δ_3 is appreciable for θ_1 smaller than 20° and becomes nearly linear

between 20° and 60°. It then approaches a saturation value of about 0.32. In Fig. 5, we have plotted the cutoff frequencies versus dielectric constant of dielectric layer for $\theta = 45°$, $\Lambda = 0.05$, $r = 1/3$, and $N = 500$. All the cutoff frequencies, in general, decrease with increasing dielectric constant. The corresponding first three gap sizes are depicted in Fig. 6, where Δ_1 decreases slowly with increasing dielectric constant. A peak value in Δ_2 is attained for $\varepsilon_{r3} = 5$, and then decreases as the dielectric constant increases. As for Δ_3, it also attains a maximum when $\varepsilon_{r3} = 10$, and Δ_3 is equal to Δ_1 for $\varepsilon_{r3} = 3$.
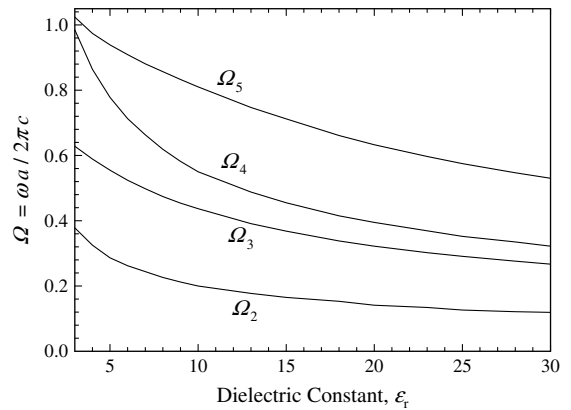

Fig. 5. Calculated four cutoff frequencies as a function of dielectric constant. The conditions are $\theta_1 = 45°$, $\Lambda = 0.05$, $r = 1/3$, and $N = 500$.
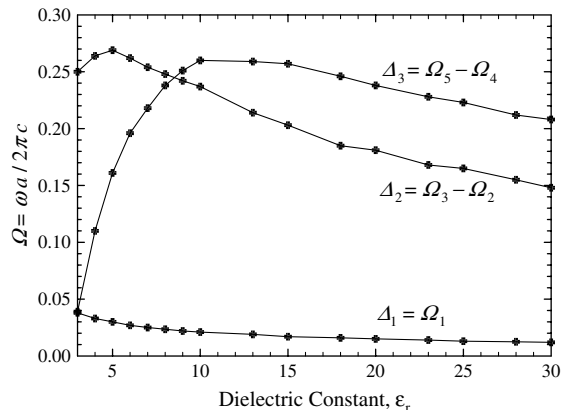

Fig. 6. The corresponding first three PBGs as a function of penetration depth calculated from Fig. 5 at the same conditions.

In the above numerical results, the calculated frequency for a superconductor photonic crystal (SPC) is normalized in $1/\lambda_0$, the sole material parameter of a superconductor involved in the formulation. This indicates that the results are valid for all the possible superconductors described by the two-fluid model [8]. Most high-T_c cuprates have a value of $\lambda_0 \approx 200$–300 nm, corresponding to infrared region. As for the conventional superconductor such as a typical A15 compound superconductor with T_c above 10 K, $\lambda_0 \approx 60$–90 nm, it then can work in the yellow to violet region. The feasibility of a SPC has been well discussed by Feng et al. [14].

4. Summary

By using the Abeles theory for a stratified medium and two-fluid model for a superconductor, we have calculated the TE mode transmittance spectrum for a superconductor-dielectric superlattice. We have also presented the photonic band structure based on the transfer matrix method together with the Bloch theorem. Results show excellent agreement for both methods. From the calculated results, some conclusions can be drawn as follows: For a one-dimensional superconducting photonic crystal, the band structure shows a multiple-PBG structure, not just the first band as shown previously in Ref. [8]. The fundamental difference is the existence of the low-frequency band gap which is not shown in all-dielectric photonic crystals. This gap is a true PBG, whereas it is not a PBG for a metallic photonic crystal. Besides the first band gap, we also have investigated the second and third PBGs as a function of penetration depth, angle of incidence, and permittivity of dielectric. The results reveal more basic information for the electromagnetic response of superconductor and

it could be of technical use in superconducting electronics.

Acknowledgements

References

[1] E. Yablonovitch, Phys. Rev. Lett. 58 (1987) 2059.
[2] S. John, Phys. Rev. Lett. 58 (1987) 2486.
[3] J.D. Joannopoulos, R.D. Meade, J.N. Winn, Photonic Crystals, Princeton University Press, New Jersey, 1995, p. 41.
[4] M.M. Sigalas, R. Biswas, K.M. Ho, C.M. Soukoulis, D.D. Crouch, Phys. Rev. B 60 (1999) 4426.
[5] V. Kuzmaik, A.A. Maradudin, Phys. Rev. B 55 (1997) 7427.
[6] A.R. McGurn, A.A. Maradudin, Phys. Rev. B 48 (1993) 17576.
[7] H. Takeda, K. Yoshino, A.A. Zakhidov, Phys. Rev. B 70 (2004) 085109.
[8] C.H. Raymond Ooi, T.C. Au Yeung, C.H. Kam, T.K. Lim, Phys. Rev. B 61 (2000) 5920.
[9] C.H. Raymond Ooi, T.C. Au Yeung, Phys. Lett. A 259 (1999) 413.
[10] Pochi Yeh, Optical Waves in Layered Media, Wiley, New York, 1988 (Chapter 6).
[11] M. Born, E. Wofl, Principles of Optics, Cambridge, London, 1999.
[12] T. van Duzer, C.W. Turner, Principles of Superductive Devices and Circuits, Edward Arnold, London, 1981.
[13] R.D. Meade, K.D. Brommer, A.M. Rappe, J.D. Joannopoulos, Phys. Rev. B 44 (1991) 13772;
R.D. Meade, K.D. Brommer, A.M. Rappe, J.D. Joannopoulos, Phys. Rev. B 44 (1991) 10961.
[14] L. Feng, X.-P. Liu, J. Ren, Y.-F. Tang, Y.-B. Chen, Y.-F. Chen, Y.-Y. Zhu, J. Appl. Phys. 97 (2005) 073104.